DOI:10.21276/sjeat.2016.1.4.4

Saudi Journal of Engineering and Technology
Scholars Middle East Publishers
Dubai, United Arab Emirates
Website: http://scholarsmepub.com/

ISSN 2415-6272 (Print)
ISSN 2415-6264 (Online)

Research Article

Modeling and Simulation Issues On Standalone Two Axis Sun Tracker

Farhan A. Salem[2], Ahmad A. Mahfouz [1]
[1]Dept. of Automatic and Mechatronics Systems, Vladimir State University, Vladimir, RF
[2]Alpha Center for Engineering Studies and Technology Researches (ACESATR), Amman, Jordan.

***Corresponding Author:**
Farhan A. Salem
Email: salem_farh@yahoo.com

Abstract: This paper proposes a new model for design of standalone two axis sun-tracker (SATAST) and some considerations regarding design, modeling and control solutions. Proposed overall system model and sub-models are developed to allow designer to have maximum numerical visual and graphical data to select, test and analyze a given SATAST system for desired output performance and characteristics, under given input operating conditions, to meet desired outputs for specific application requirements.
Keywords: Photovoltaic (PV) system, 2D suntracker Modeling, simulation.

INTRODUCTION

With the growing requirements to improve fuel consumption economy and reduce related emissions, solar energy became the world's major renewable energy source; it is a clean, available everywhere in different quantities and renewable with a long service life, high reliability, little operation and maintenance costs. Solar energy is directly converted into electrical energy by solar PhotoVoltaic (PV) system. PV system is a whole assembly of solar cells, connections, protective parts, supports etc. The basic device of a PV system is the single PV cell. Each individual cell is a functioning power generating device[1]. Fragile cells are hermetically sealed under toughened, high transmission glass to produce highly reliable, weather resistant modules that may be warranted for up to 25 years .The power produced by a single PV cell is not enough for general use, where, each solar cell generates approximately 1.75 watts (0.5V DC and amps) and converts only 12 to 20 % of the sun's light into electricity, Therefore, in most commercial PV products, PV cells are generally connected in series configuration to form a PV module (the fundamental building block of PV systems) in order to obtain adequate working voltage, generally of 36-cells to charge a 12V battery and similarly a 72-cell module is appropriate for a 24V battery. PV modules are then arranged in series-parallel structure (series connections for high voltage requirement and in parallel connections for high current requirement) to form PV panels (consisting of one or more PV modules) to produce enough high power to achieve desired power output [2]. Panels can be grouped to form large photovoltaic arrays. The term *array* is usually employed to describe a complete power-generating unit, consisting of any number of PV modules and panels. The performance (output characteristics) of a PV array system depends on the operating conditions, as well as, the solar cell and array design quality, where the output voltage, current and power of PV array system vary as functions of solar irradiation level β, temperature T , voltage V, and load current I. the effects of these three quantities must be considered in the design of PV array systems, so that any change in temperature and solar irradiation levels should not adversely affect the PV array output to the load/utility, which is either a power company utility grid or any stand alone electrical type load [3].

A PV cell is basically a semiconductor diode whose *p–n* junction is exposed to light [4]. The mono-crystalline and multi-crystalline silicon cells are the only found at commercial scale at the present time. The PV phenomenon may be described as the absorption of solar radiation, the generation and transport of free carriers at the *p–n* junction, and the collection of these electric charges at the terminals of the PV device [5-6]. The rate of generation of electric carriers depends on the flux of incident light and the capacity of absorption of the semiconductor. The capacity of absorption depends mainly on the semiconductor bandgap, on the reflectance of the cell surface (that depends on the shape and treatment of the surface), on the intrinsic concentration of carriers of the semiconductor, on the electronic mobility, on the recombination rate, on the temperature, and on several other factors [3]

The current rating of the PV cell-system increases when the area of the individual cells is increased [7]. The power generated by any solar cell is a function of three variables: the surface area of the cell exposed to light, the efficiency of the cell, and an environmental constant known as *irradiance*, the best way to increase power generation would be to increase exposed surface area, also for optimal operational efficiency of solar energy receivers, and correspondingly generated electricity, solar tracking systems are designed such that solar panels are perpendicular to sunlight, where the illumination is strongest, to achieve this, an ideal tracker would compensate for changes in both sun's altitude and latitudinal angles through both day and seasonal changes and changes in azimuth angle. In 1986, Akhmedyarov first increased the output power of a solar photoelectric station in Kazakhstan from 357W to 500W by integrating the station with an automatic sun tracking system [8],also studies show that, a solar panel of $3m^2$ with fixed position to surface produces about 5 kWh of electricity per day, the same installation but equipped with tracker, can provide up to 8 kWh per day. Several methods and designs of sun tracking systems have been proposed, designed and implemented, main are included in [7-16]. a detailed literature review can be found in [16]

This paper proposes modeling, simulation and control issues for Mechatronics design of standalone two axis sun-tracker (SATAST), the SATAST system consists of five main subsystems including; PV panel for power generation, DC/DC converter for power conditioning, actuating units responsible for motions, control units, sensing unit, each subsystem, to be mathematically described and corresponding Simulink sub-model developed, then an integrated design of all subsystem is to be developed, the subsystems models and the whole SATAST system model, are to be tested and analyzed for desired system requirements and performance**.** SATAST sub-systems arrangements is shown in Figure 1(a)(b)**.**

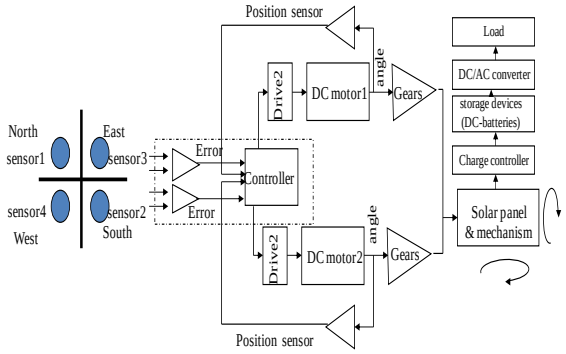

Fig-1(a): Two axis solar tracker system arrangements

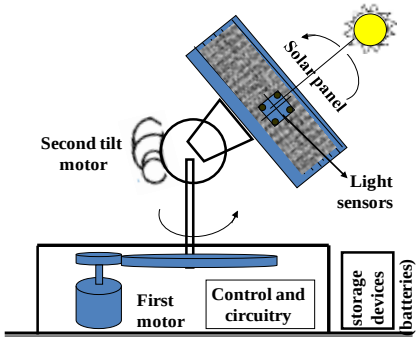

Fig-1(b): Proposed SATAST system design

Modeling and simulation of SATAST system

The SATAST system consists of five main subsystems in particular; PV panel, DC/DC converter, actuating units, control units and sensing units, each subsystem, to be mathematically described and corresponding Simulink sub-model developed, then an integrated design of all subsystem is to be developed, the subsystems models and the whole SATAST system model, are to be tested and analyzed for desired system requirements and performance

Modeling and simulation of the PV system

A general mathematical description of I-V output characteristics for a PV cell has been studied for over the last four decades and can be found in different resources including, but not limited to [1, 2, 5, 6, 17, 18]**.** Solar (photovoltaic) cells consist of a p-n junction fabricated in

a thin wafer or layer of Mono-crystalline or multi-crystalline silicon semiconductor. PV system naturally exhibits a nonlinear I-V and P-V output characteristics which vary with irradiation level β, cell temperature T , voltage V, and load current I. In the dark, the I-V output characteristic of a solar cell has an exponential characteristic similar to that of a diode [18]. When solar energy (photons) hits the solar cell, with energy greater than bandgap energy of the semiconductor, electrons are knocked loose from the atoms in the material, creating electron-hole pairs [17]. These carriers are swept apart under the influence of the internal electric fields of the *p-n* junction and create a current proportional to the incident radiation. When the cell is short circuited (zero load resistance), this current flows in the external circuit; when open circuited, this current is shunted internally by the intrinsic *p-n* junction diode. The characteristics of this diode therefore set the open circuit voltage characteristics of the PV solar cell [18]. Based on this the simplest equivalent circuit of a PV solar cell consists of a diode, a photo current, a parallel resistor expressing a leakage current, and a series resistor describing an internal resistance to the current flow, all as shown in Figure 2(a), this equivalent circuit is called a *single diode* model. The diode determines the I-V characteristics of the cell [19] more exact mathematical description of a PV cell, so called the *double (exponential)* diode model shown in Figure 2(b) [20] is derived from the physical behavior of PV solar cell constructed from polycrystalline silicon. This model is composed of a light-generated current source, two diodes, a series resistance and a parallel resistance. However, there are some limitations to develop expressions for the V-I curve parameters subject to the implicit and nonlinear nature of the model, therefore, this model is rarely used in the subsequent literature and is not taken into consideration. A model of PV solar cell with suitable complexity is shown in Figure 2(c), since a small variation in series resistance R_S will significantly affect the PV output power, and the PV efficiency is insensitive to variation in shunt resistance R_{SH} ,therefore the effect of R_{SH} can be neglected, and correspondingly, a simplified model is shown in Figure 2(d) [21] where R_S effect becomes very conspicuous in a PV module that consists of many series-connected cells, and the value of resistance is multiplied by the number of cells, meanwhile R_{SH} will only become noticeable when a number of PV modules are connected in parallel for a larger system.

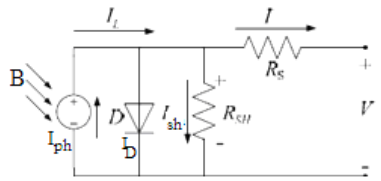

Fig-2 (a): Single diode (exponential) model of the PV model.

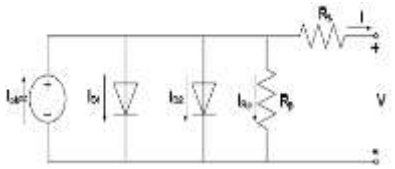

Fig-2 (b): PV Double diode (exponential) model

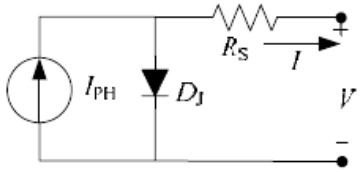

Fig-2(c): Single diode (Appropriate,) model of PV Cell

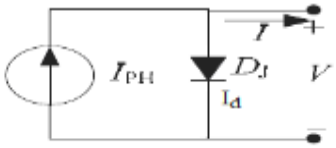

Fig-2(d): PV *Simplified Ideal* single diode model

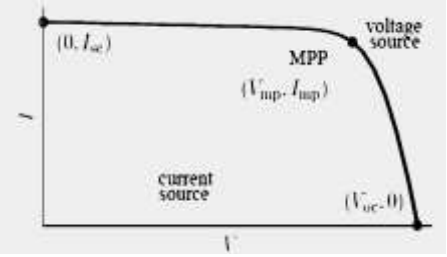

Fig-2(e): Characteristic I-V curve of a practical photovoltaic device and the three *remarkable points*: short circuit *(0, I_{sc})*, maximum power point *(V_{mp}, I_{mp})* and open-circuit*(V_o, 0)*[1]

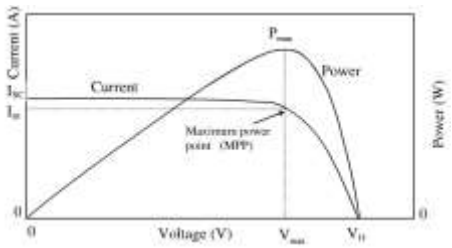

Fig-2(f): Typical characteristic I-V and P-V curve of a practical photovoltaic device and the three *remarkable points* [1]

Photovoltaic Panel –Converter (PVPC) subsystem model

The PVPC system consists of two main subsystems; PV panel and DC/DC converter with battery subsystems. The PV panel is used as electricity generator to convert the irradiance from sunlight into electricity using photovoltaic system to generate its own power for motion and for storing in batteries, and use power converter as a device that converts electrical energy source by switching devices

Photovoltaic cell-Panel subsystem modeling

A general mathematical description of a PV cell in terms of output voltage, current, power and of I-V and P-V characteristics has been studied for over the past four decades and can be found in different resources, many of which are listed in [24]. ***The output net current of PV cell I***, and the V-I characteristic equation of a PV cell are given by Eq.(39), it is the difference of three currents; the light-generated *photocurrent* I_{ph}, *diode* current I_d and the *shunt* current I_{RSH}. The output voltage, current and power of PV array vary as functions of solar irradiation level β, temperature T , cell voltage V and load current I, where with *increase* in temperature at *constant* irradiation, the power output *reduces*, also, by increasing operating temperature, the current output increases and the voltage output reduces, similarly with irradiation. Therefore the effects of these three quantities must be considered in the design of PV arrays so that any change in temperature and solar irradiation levels should not adversely affect the PV array output to the load/utility [24].

$$
\begin{aligned}
I &= I_{ph} - I_d - I_{RSH} \\
I &= I_{ph} - I_s\left(e^{\frac{q(V+IR_S)}{NKT}} - 1\right) - \frac{V + R_S I}{R_{sh}} \\
I &= \left(I_{sc} + K_i\left(T - T_{ref}\right)\right)\frac{\beta}{1000} - I_s\left(e^{\frac{q(V+IR_S)}{NKT}} - 1\right) - \frac{V + R_S I}{R_{sh}}
\end{aligned}
\qquad (39)
$$

Based on these equation and in reference to [25-26], Simulink model shown in Figure 3(a)(b) of PV cell-array are developed, this model this model is developed to allow designer to have maximum numerical visual and graphical data to select, test and analyze a given PV system for desired output performance and characteristics under given operation condition, including; cell's-panels current, voltage, powers, efficiency and fill factor.

Running model given in Figure 3(d), for PV parameters defined in Table 1, at standard operating conditions of irradiation $\beta=1000$, and $T=25$, will result in P-V and I-V characteristics shown in Figure 3(c)(d) and shown visual numerical values of cell's-panels current, voltage, powers, efficiency and fill factor, these curves show that, this is 3.926 Watt PV cell with I_{SC} = *8.13 A* , *Vo= 0.6120V* , I_{max} *=7.852 A* , V_{max} *=0.5 V, (MPP =* I_{max} * V_{max} *=7.852 *0.5=3.926).*

DC/DC Converter subsystem modeling

In this paper step-down DC/DC *Buck converter* is used. Referring to [23] *Buck converter* circuit diagram, Simulink model and mask shown in Figure 4 (a)(b)(c) are introduced, as well as Photovoltaic panel-Converter (PVPC) system Simulink model, shown in Figure 4(d)(e). These Figures show the outputs of both PVPC subsystems when tested for defined parameters listed in Table-1

including duty cycle of D=0.5. Duty cycle is the ratio of output voltage to input voltage is given by Eq.(40), Where: I_{out} and I_{in}, : the output and input currents. D : the duty ratio (cycle) and defined as the ratio of the ON time of the switch to the total switching period. In this paper, the PWM generator is assumed as ideal gain system, the duty cycle of the PWM output will be multiplied with gain $Kv = K_D$, This equation shows that the output voltage of buck converter is lower than the input voltage; hence, the duty cycle is always less than 1.

$$\frac{V_{out}}{V_{in}} = D = \frac{I_{in}}{I_{out}} \Rightarrow V_{out} = D * V_{in} \Leftrightarrow D = \frac{T_{on}}{T_{on} + T_{off}} \quad (40)$$

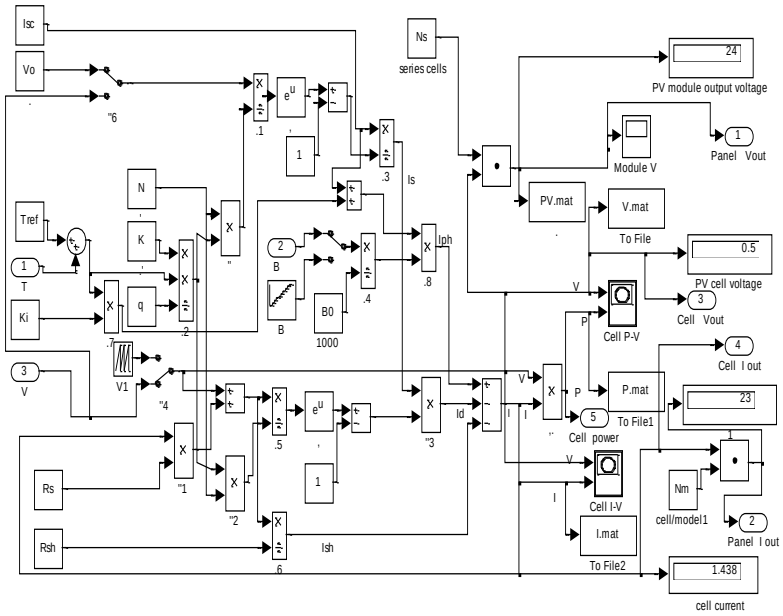

Fig-3(a): PV cell (module) Simulink subsystem model [22].

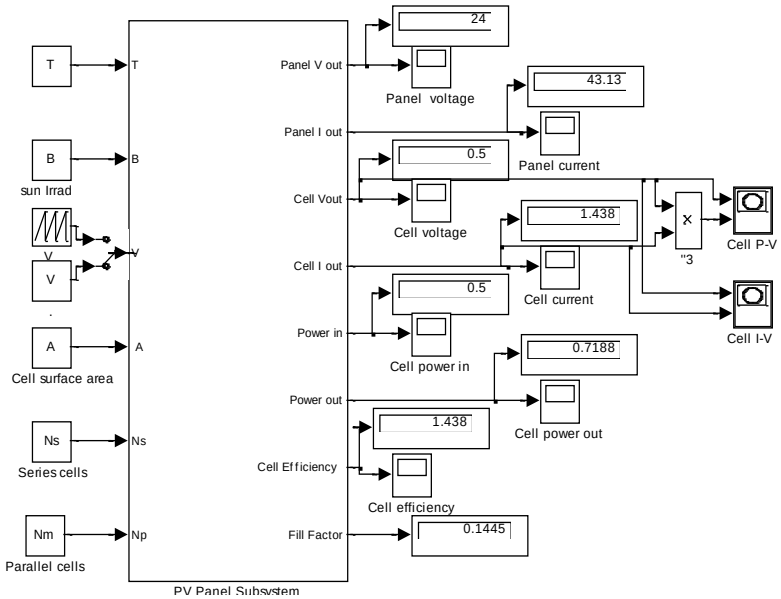

Fig-3(b): Generalized PV Cell (module) Simulink model

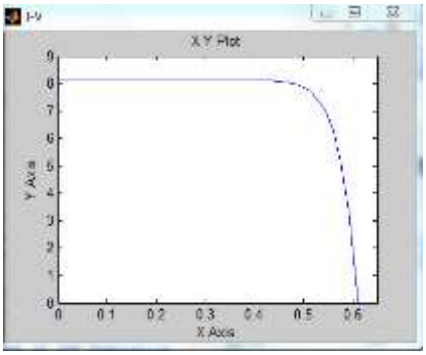

Fig-3(c): V-I Characteristics for β=1000, and T=25

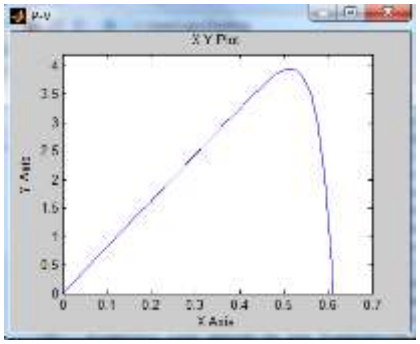

Fig-3(d): P-V Characteristics for β=1000, and T=25

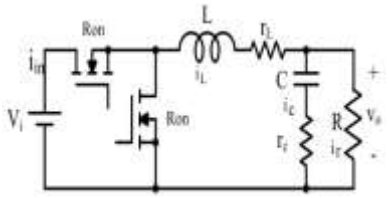

Fig-4(a): Buck converter circuit diagram [22]

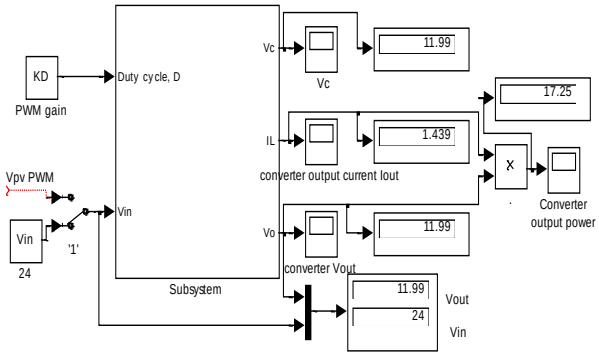

Fig-4(b): Buck converter Simulink model, based on refined math model

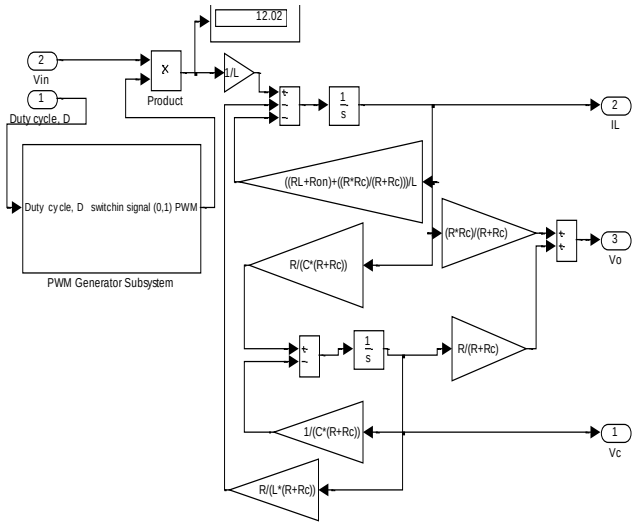

Fig-4(c): Buck converter subsystems model

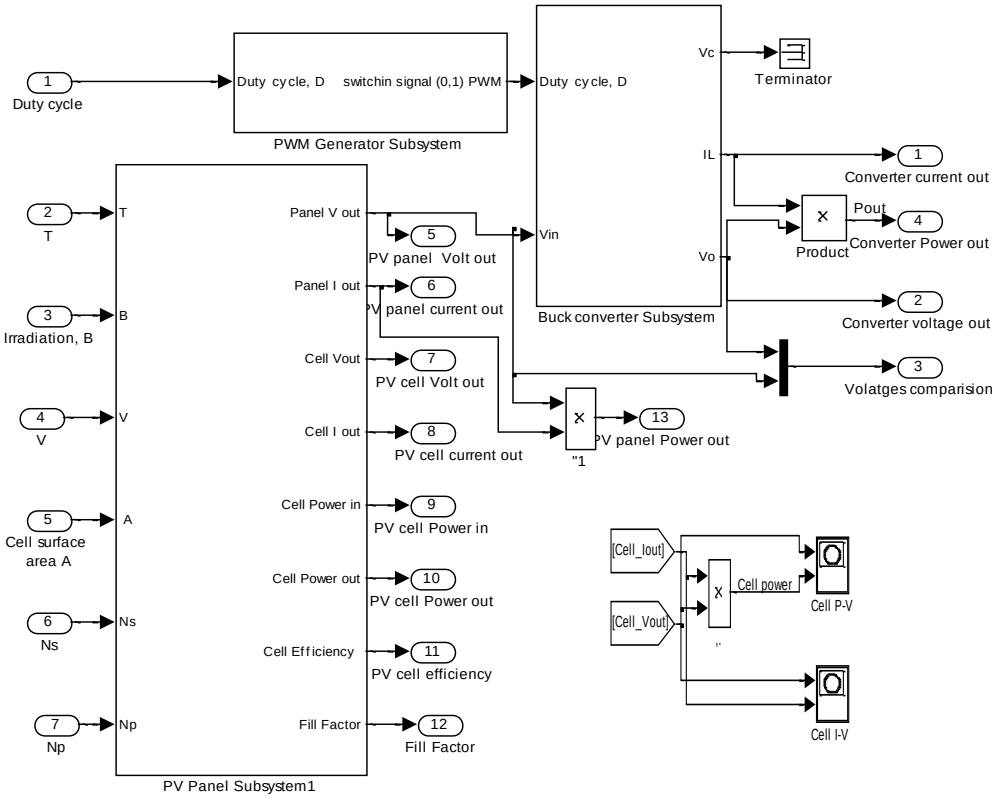

Fig-4(d): PVPC system sub-model consisting of three subsystems; PV panel, converter and PWM sub-models

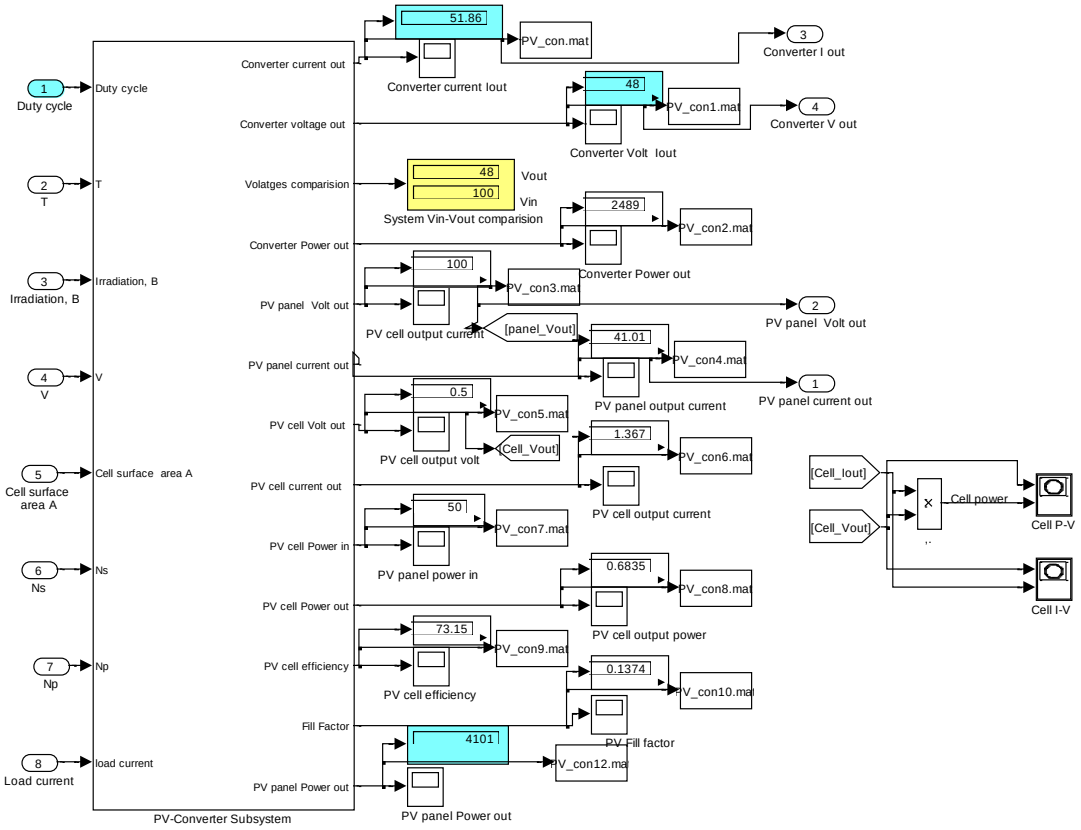

Fig-4(e): PVPC system model with all subsystems

Control unit subsystem selection, modeling and design

Different control approaches can be proposed to control the overall SAST system output performance in terms of output position, as well as, controlling output characteristics and performance of PVPC subsystem to meet desired output voltage or current under input working operating conditions. because of its simplicity and ease of design, PI controller is widely used in variable *speed* applications and *current* regulation, in this paper PI controller is selected for achieving desired outputs characteristics of PVPC subsystem and meeting desired output speed of overall SEMRP system, where Different PI controllers configurations are to be applied to control the PVPC subsystem and overall SEMRP system to achieve desired outputs of speed, voltage and load currents for particular SEMRP system application, notice that PI controller can be replace with PID or any other suitable control algorithm.

The *PI* controller transfer function in different forms is given by Eq.(41). The PI controller pole and zero will affect the response, mainly the PI zero given by; Z_o=-K_I/K_P, will inversely affect the response and should be canceled by prefilter, while maintaining the proportional gain (K_P), the prefilter transfer function is given by Eq.(42) , the placement of prefilter is shown on generalized model.

$$G_{PI}(s) = K_P + \frac{K_I}{s} = \frac{(K_P s + K_I)}{s} = \frac{K_P\left(s + \frac{K_I}{K_P}\right)}{s} = \tag{41}$$

$$= \frac{K_P(s+Z_o)}{s} = G_{PI}(s) = K_{PI} * \frac{(T_I s + 1)}{T_I s} = K_{PI} * \left(1 + \frac{1}{T_I s}\right)$$

$$G_{Prefilter}(s) = \frac{Z_O}{(s+Z_O)} = \frac{Z_{PI}}{(s+Z_{PI})} \tag{42}$$

Electric motor sub-system modeling

Solar tracking system motion control is simplified to an electric motor motion control, in terms of output angular displacement; therefore, the conception of solar tracking system can be presented as position control of one eclectic motor, considering that, the system operation is accomplished by one of two used two motors.

The DC motor open loop transfer function without any load attached relating the input voltage, $V_{in}(s)$, to the output angular displacement, $\theta(s)$, is given by Eqs(1)(2). The total equivalent inertia, J_{equiv} and total equivalent damping, b_{equiv} at the armature of the motor are given by Eq(3), for simplicity, the solar panel can be considered to be of cuboide shape, with the inertia calculated by Eq(4), also the total inertia can be calculated from the energy conservation principle, correspondingly, the equivalent STAST system transfer function with gear ratio, n, is given by Eq(5) [1]

$$G_{angle}(s) = \frac{\theta(s)}{V_{in}(s)} = \frac{K_t}{\left\{s\left[(L_a s + R_a)(J_m s + b_m) + K_t K_B\right]\right\}}$$

$$\frac{\theta(s)}{V_{in}(s)} = \frac{K_t}{\left\{\left[L_a J_m s^3 + (R_a J_m + b_m L_a)s^2 + (R_a b_m + K_t K_b)s\right]\right\}} \tag{1}$$

Armature inductance, L_a is low compared to the armature resistance, R_a (discussed later). Neglecting motor inductance by assuming, (L_a =0), manipulating and gives:

$$\frac{\theta(s)}{V_{in}(s)} = \frac{\frac{K_t}{R_a J_a}}{s\left[s + \frac{1}{J_m}\left(b_m + \frac{K_t K_b}{R_a}\right)\right]} \tag{2}$$

$$b_{equiv} = b_m + b_{Load}\left(\frac{N_1}{N_2}\right)^2 \quad \Leftrightarrow \quad J_{equiv} = J_m + J_{Load}\left(\frac{N_1}{N_2}\right)^2 \tag{3}$$

$$J_{load} = \frac{m(h^2 + a^2)}{12}, \ ,$$

$$0.5 * m_{total} * \upsilon^2 = 0.5 * J_{load} * \omega^2 \Rightarrow J_{load} = \frac{m_{total} * \upsilon^2}{\omega^2} \tag{4}$$

$$G_{angle}(s) = \frac{K_t / n}{s\left[(L_a J_{equiv})s^2 + (R_a J_{equiv} + b_{equiv} L_a)s + (R_a b_{equiv} + K_t K_b)\right]} \tag{5}$$

Based on these equations, actuator sub-system Simulink model is shown in Figure 5

SATAST system model

Integrating all subsystems in one overall SATAST system model will result in model shown in Figure 6, consisting of two DC actuators for east-west and north-south motions, PVPC subsystem with its dynamics and control units.

Testing and evaluation

Applying calculated altitude angle, for Taif city as given by [24] as the input data (error) for the designed control system, for one degree of freedom (Figure 7), will result in corresponding panel angle, plotting both input angle and output panel angle in the same graph window, will result in response curve shown in Figure 8. These response curves show that, the input and output angles curves are with small error, by soft tuning of control system, the input can match the output without error, comparison show that the solar panel tracks the sun, resulting in optimal operational efficiency of solar energy photovoltaic module.

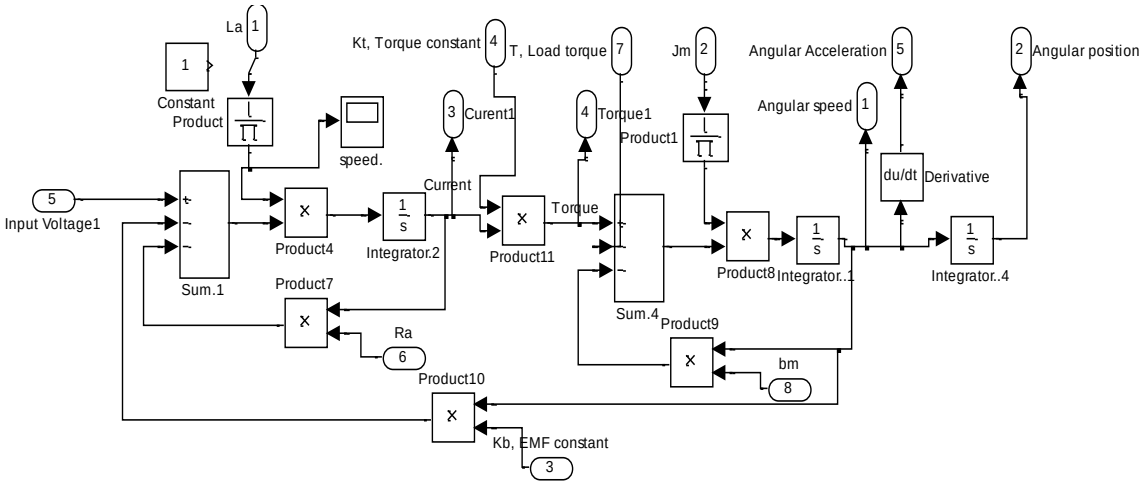

Fig-5: Actuator sub-system

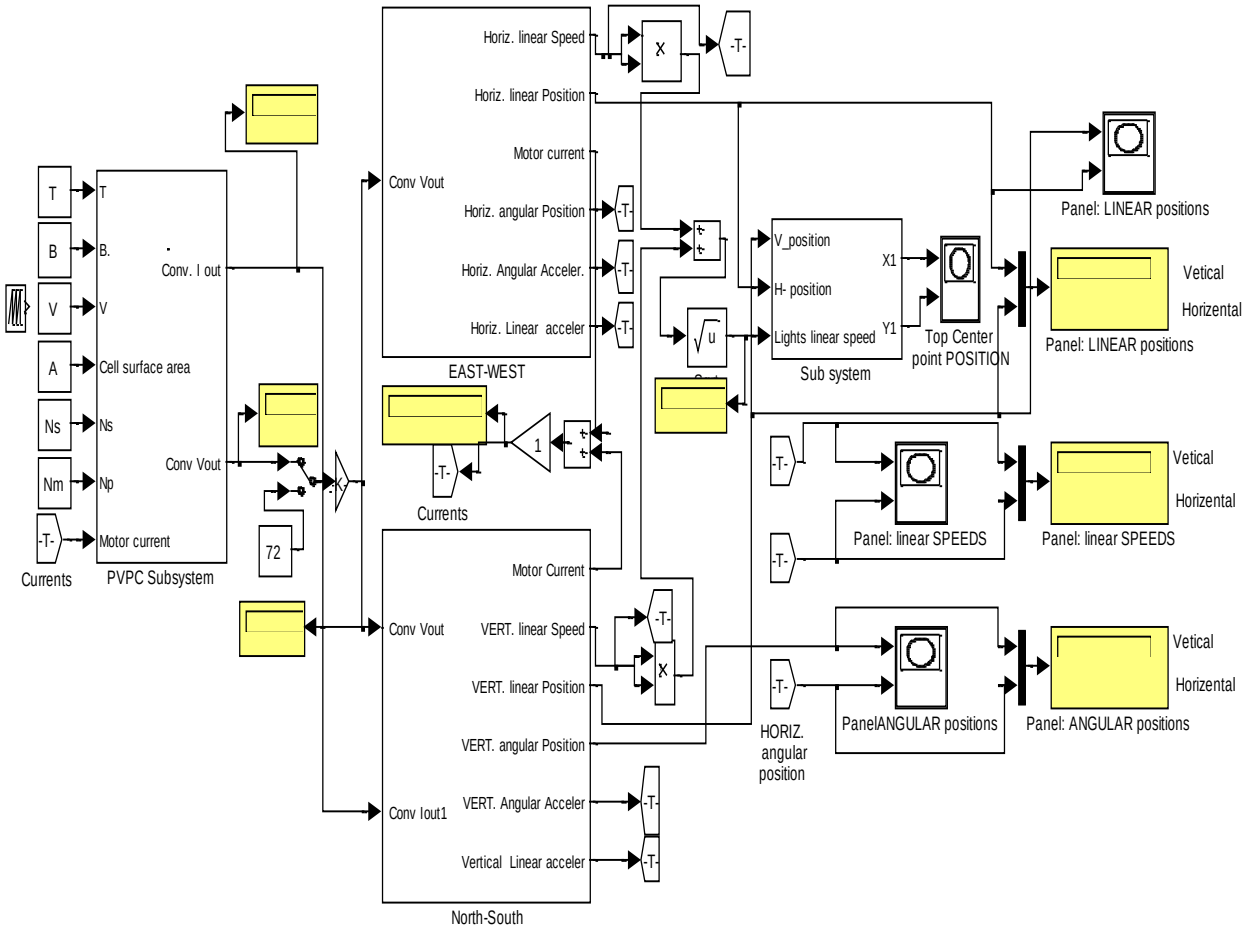

Fig-6: overall SATAST system Simulink model

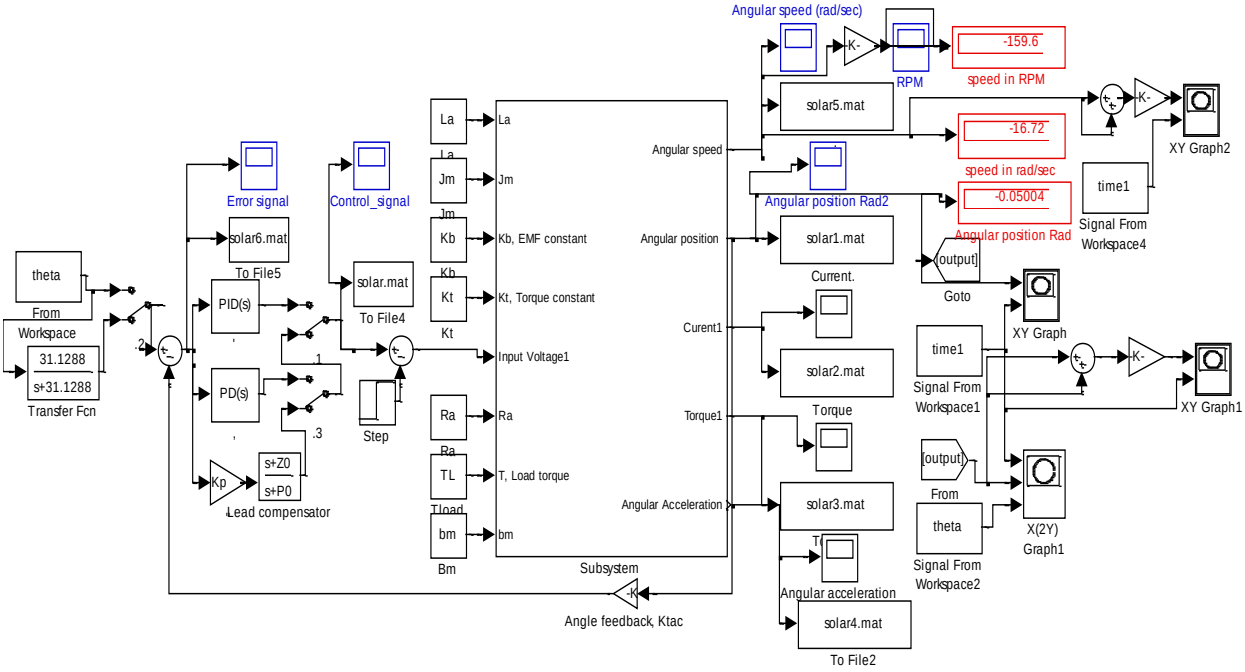

Fig-7: Simulink model of one DOF solar tracker system

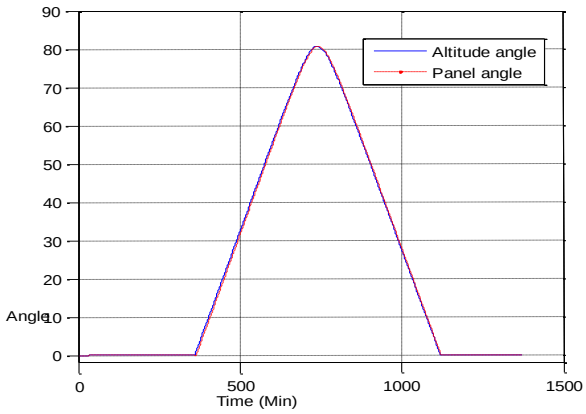

Fig-8: calculated altitude angle for Taif city, as input and resulted panel angle as system response

Running overall SATAST system model for defined parameters listed in Table-1, for one day (east-west motion with max of 90 degrees and north-south with max 4 degree) for 10 s ,will result in response curves shown in Figure 9, where in Figure 9(a) are shown PV panel output voltage (100V), and converter's output voltage (48V) and current(51.5A), these values are shown in Figure 6 (d) of PVPC system sub model. In Figure 9(b) is shown actuator angular displacement for desired 90 angles. In Figure 9(c) are shown actuator readings including linear position, speed and torque generated. Panel 2D (vertical-horizontal) linear and angular position, linear speeds and panel top center point path are shown in Figure 10.

Running overall SATAST system model for one day (east-west motion with max 180 degrees and north-south with 1 degree) , will result in Panel 2D (vertical-horizontal) linear and angular position, linear speeds and panel top center point path shown in Figure 11, depending on selected and designed control system, these response curves can be further refined.

These response curves show the simplicity and applicability of the proposed models in selecting, testing and evaluating the design of 2D suntracker, for optimal operation and power generation.

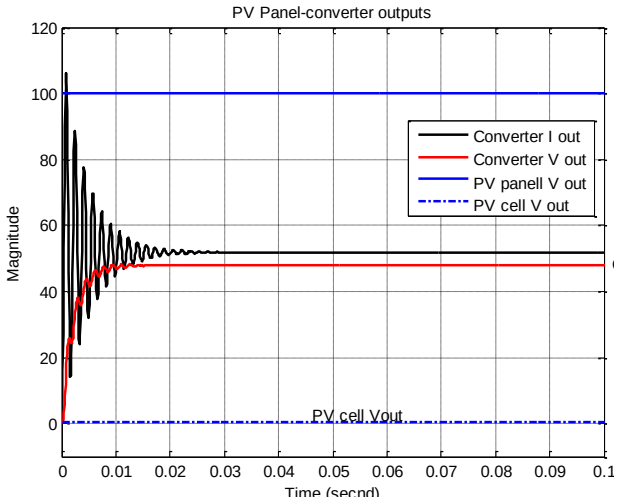

Fig-9(a): PV panel output voltage, and converter's output voltage and current

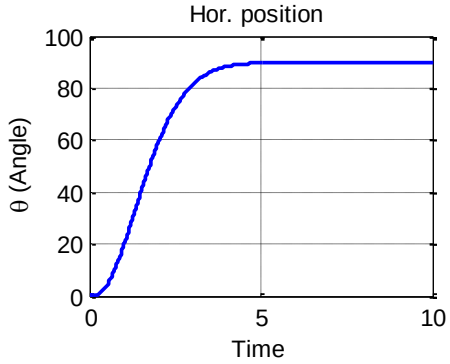

Fig-9(b): One Actuator angular displacement for 90 degrees

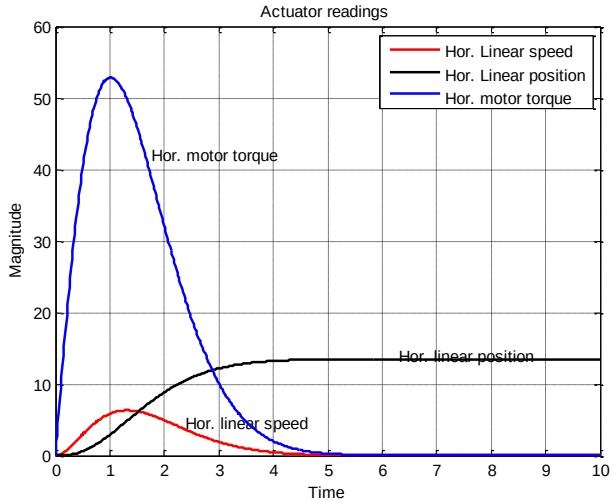

Fig-9(c): actuator readings: linear speed, position and torque

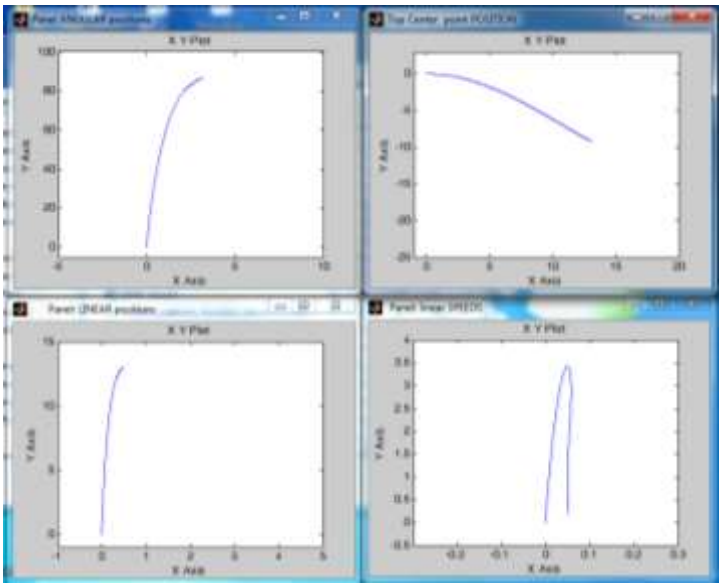

Fig-10: Panel 2D (vertical-horizontal) linear and angular positions, linear speeds and panel top center point track (east-west with max of 90 degrees and north-south with max 4 degree)

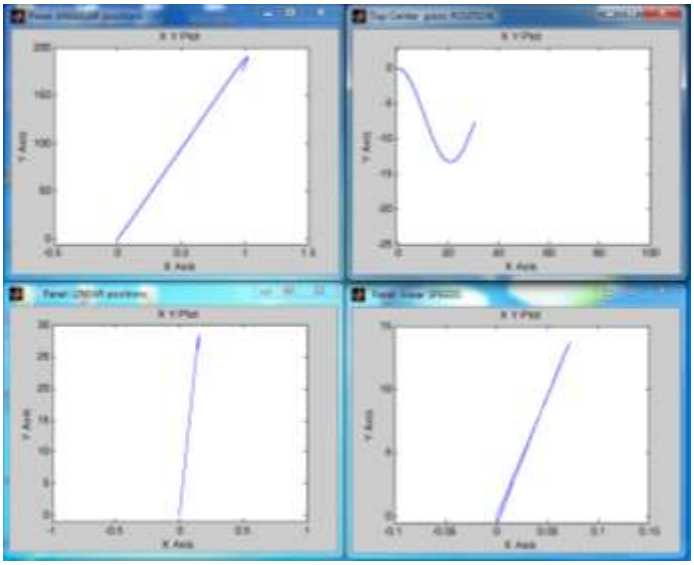

Fig-11: Panel 2D (vertical-horizontal) linear and angular positions, linear speeds and panel top center point track (One day east-west with max of 180 degrees and north -south with max 1 degree)

CONCLUSIONS

A new model for Mechatronics design of standalone suntracker and some considerations regarding design, modeling and control are proposed. The proposed SATAST system model consists of five main subsystems, each subsystem, is mathematically described and corresponding Simulink sub-model is developed, then an generalized whole SATAST system model is developed by integrating all sub-models, the generalized model is developed to allow designer to have the maximum output data (numerical and graphical) to select, test and evaluate the overall SATAST system and each subsystem outputs characteristics and performance, under various PV subsystem input operating conditions, to meet particular requirements and performance. The obtained results show the simplicity, accuracy and applicability of the presented designs and models to help in Mechatronics design of SATAST system .

L_a=0.82 MH	Motor armature Inductance,
J_m=0.271 kg.m^2	Geared-Motor Inertia
b_m=0.271 N.m.s	Viscous damping
K_b=1.185 rad/s/V	Back EMF constant,
n=1	Gear ratio
J_{equiv} kg.m^2	The total equivalent inertia,
b_{equiv} N.m.s	The total equivalent damping,
K_{pot} =0.2667	Tachometer constant, for right-left motion
K_{pot}1=0.0.5333	Tachometer constant, for up-dawn motion
ω=speed/r, rad/s	Shaft angular speed rad/sec
T_{shaft}	The torque produced by motor
η	The transmission efficiency
T_{shaft}	The torque, produced by the driving motor
Solar cell parameters	
Isc=8.13 A , 2.55 A , 3.8	The short-circuit current, at reference temp 25°C
I A	The output net current of PV cell (*the* PV *module current*)
I_{ph} *A*	The light-generated *photocurrent* at the nominal condition (25°C and 1000 W/m^2),
E_q *: =1.1*	The band gap energy of the semiconductor
$V_t = KT/q$	The thermo voltage of cell. For array :($V_t = N_s KT/q$)
I_s ,*A*	The reverse saturation current of the diode or leakage current of the diode
Rs=0.001 Ohm	The series resistors of the PV cell, it they may be neglected to simplify the analysis.
Rsh=1000 Ohm	The shunt resistors of the PV cell
V	The voltage across the diode, output
q=1.6e-19 C	The electron charge
B_o*=1000 W/m^2*	The Sun irradiation
β =B=200 W/m^2	The irradiation on the device surface
Ki=0.0017 A/∘C	The cell's short circuit current temperature coefficient
Vo= 30.6/50 V	Open circuit voltage
Ns= 48 , 36	Series connections of cells in the given photovoltaic module
Nm= 1 , 30	Parallel connections of cells in the given photovoltaic module
K=1.38e-23 J/oK;	The Boltzmann's constant
N=1.2	The diode ideality factor, takes the value between 1 and 2
T= 50 Kelvin	Working temperature of the *p-n* junction
T_{ref}*=273 Kelvin*	The nominal reference temperature
Buck converter parameters	
C=300e-6; 40e-6 F	Capacitance
L=225e-6 ; .64e-6 H	Inductance
Rl=RL=7e-3	Inductor series DC resistance
rc= RC=100e-3	Capacitor equivalent series resistance, ESR of C ,
V_{in}*= 24 V*	Input voltage
R=8.33; 5 Ohm;	Resistance
Ron=1e-3;	Transistor ON resistance
KD=D= 0.5, 0.2,	Duty cycle
Tt=0.1 , 0.005	Low pass Prefilter time constant
V_L	Voltage across inductor
I_C	Current across Capacitor

REFERENCES

1. Farhan A. Salem (2014), Modeling and Simulation issues on PhotoVoltaic systems, for Mechatronics design of solar electric applications, IPASJ International Journal of Mechanical Engineering (IIJME) Volume 2, Issue 8, August.
2. Huan-Liang Tsai, Ci-Siang Tu, and Yi-Jie Su,(2008) Development of Generalized Photovoltaic Model Using Matlab/Simulink, Proceedings of the World Congress on Engineering and Computer Science, October 22 - 24, 2008, San Francisco, USA
3. J. Surya Kumari, Ch. Sai Babu(2012), Mathematical Modeling and Simulation of Photovoltaic Cell using Matlab-Simulink Environment, International Journal of Electrical and Computer Engineering (IJECE) Vol. 2, No. 1, pp. 26~34 February ,
4. Sergio Daher, Jurgen Schmid and Fernando L.M Antunes(2008), "Multilevel Inverter Topologies for Stand- Alone PV Systems*" IEEE Transactions on Industrial Electronics*.Vol.55, No.7, July .
5. Soeren Baekhoeg Kjaer, John K.Pedersen Frede Blaabjerg(2005) "A Review of Single –Phase Grid-Connected Inverters for Photovoltaic Modules" *IEEE Transactions on Industry Appications*, Vol.No.5, September/October .J.M.A. Myrzik and M.Calais(2003) "*Sting and Module Intigratrd Inverters for Single –Phase Grid-Connected Photovoltaic Systems – Review*" IEEE Bologna Power Tech conference, June .
6. Mohammed S. El-Moghany, Basil M. Hamed (2012), Two axis tracker using fuzzy controller via PIC16F887a, *The 4th International Engineering Conference –Towards engineering of 21st century.*
7. Akhmedyarov, K.A.; Bazarov, B.A.; Ishankuliev. B.; Karshenas, K.E.; Schaimerdangulyev G. (1986), Economic efficiency of the FV-500 solar photoelectric station with automatic tracking of the sun. *Appl. Solar Energ.22*, 44-47.
8. C.S. Chin (2012), Model-Based Simulation of an Intelligent Microprocessor-Based Standalone Solar Tracking System.
9. C.S. Chin (2012), Model-Based Simulation of an Intelligent Microprocessor-Based Standalone Solar Tracking System.
10. Ahmad Rhif (2011), A position control review for photovoltaic system, Dual axis sun tracker, *IETE Technical Review* ,Volume 28, Issue 6 ,p. 479-485.
11. R. Messenger and J. Ventre (2000), Photovoltaic Systems Engineering, *CRC Press*.
12. S.A. Kalgirou (1996), Design and construction of a one axis sun-tracking system, *sol. Energy*, vol. 57, pp 459-9.
13. Gustavo Ozuna, Carlos Anaya. Diana Figueroa. Nun Pitalua (2011), Solar Tracker of Two Degrees of Freedom for Photovoltaic Solar Cell Using Fuzzy Logic, *Proceedings of the World Congress on Engineering 2011* Vol II WCE 2011, July 6 – 8,London, U.K.
14. A. Stjepanovic, F. Softic, Z. Bundalo and S. Stjepanovic (2010), Solar Tracking System and Modelling of PV Module , *MIPRO*,Opatija, Crotia.
15. A. Louchene, A. Benmakhlouf and A. Chaghi (2007), Solar Tracking System with Fuzzy Reasoning Applied to Crisp Sets , *Revue des Energies Renouvelables*, Vol. 10, No2, pp. 231 – 240.
16. Lorenzo, E. (1994). Solar Electricity Engineering of Photovoltaic Systems. Artes Graficas Gala, S.L., Spain.
17. G. Walker,(2001) "Evaluating MPPT converter topologies using a MATLAB PV model," Journal of Electrical & Electronics Engineering, Australia, IEAust, vol.21, No. 1, , pp.49-56.
18. Francisco M. González-Longatt(2005), Model of Photovoltaic Module in Matlab , 2DO Congreso Iberoamericano de estudiantes de ingeneria electrica, electronica y Computacion (II CIBELEC 2005)
19. J. A. Gow and C. D. Manning, (1999)"Development of a photovoltaic array model for use in power-electronics simulation studies," *IEE Proceedings- Electric Power Applications*, vol. 146, no. 2, , pp. 193-199.
20. Altas. I, A. M. Sharaf, (2007) "A photovoltaic array (PVA) simulation model to use in Matlab Simulink GUI environment." IEEE I-4244-0632 - 03/07.
21. N. Pongratananukul and T. Kasparis(2004). Tool for automated simulation of solar arrays using general-purpose simulators. In *Proc. IEEE Workshop on Computers in Power Electronics*, p. 10–14,.
22. J. A. Gow and C. D. Manning(1996). Development of a model for photovoltaic arrays suitable for use in simulation studies of solar energy conversion systems. In *Proc. 6th International Conference on Power Electronics and Variable Speed Drives*, p. 69–74,.
23. Ashraf Balabel, Ahmad A. Mahfouz, Farhan A. Salem (2013), Design and Performance of Solar Tracking Photo-Voltaic System; Research and education, international journal of control, automation and systms vol. , no. , april